Relativistic treatment of hypernuclear decay

L. Zhou and J. Piekarewicz

Department of Physics and Supercomputer Computations Research Institute, Florida State University, Tallahassee, Florida 32306

We compute for the first time the decay width of Λ-hypernuclei in a relativistic mean-field approximation to the Walecka model. Due to the small mass difference between the Λ-hyperon and its decay products—a nucleon and a pion—the mesonic component of the decay is strongly Pauli blocked in the nuclear medium. Thus, the in-medium decay becomes dominated by the nonmesonic, or two-body, component of the decay. For this mode, the Λ-hyperon decays into a nucleon and a spacelike nuclear excitation. In this work we concentrate exclusively on the pionlike modes. By relying on the analytic structure of the nucleon and pion propagators, we express the nonmesonic component of the decay in terms of the spin-longitudinal response function. This response has been constrained from precise quasielastic $(\vec{p},\vec{n})$ measurements done at LAMPF. We compute the spin-longitudinal response in a relativistic random-phase-approximation model that reproduces accurately the quasielastic data. By doing so, we obtain hypernuclear decay widths that are considerably smaller—by factors of 2 or 3—relative to existing nonrelativistic calculations. [S0556-2813(99)01208-X]

PACS number(s): 21.80.+a, 21.60.−n, 14.20.Jn

I. INTRODUCTION

Understanding modifications to hadronic properties—such as masses and decay widths—in the nuclear medium occupies an important place in nuclear physics. The reason for such a status is the universal character of the problem. In electromagnetic phenomena one asks, for example, if the coupling of the photon to the proton gets modified in the nuclear environment. Similarly, hadronic processes—such as the $(\vec{p},\vec{n})$ reaction—search for evidence for new states of matter through the modifications of meson (e.g., pion) properties in the nuclear medium. Finally, the modification of masses and decay widths for vector mesons might provide, through relativistic heavy-ion experiments, conclusive evidence for the formation of the quark-gluon plasma.

In the present paper we are interested in understanding medium modifications to the properties of the lambda-hyperon; in particular modifications to its decay width. To our knowledge, this is the first time that such a study will be carried out within the framework of a relativistic mean-field approximation. There are several reasons why the Λ-decay is interesting. First, the mesonic mode, $\Lambda \rightarrow N\pi$, which comprises nearly 100% of the decay in free space, is unavailable in the medium because of Pauli blocking [1]. Second, a new nucleon-stimulated mode, $\Lambda N \rightarrow NN$, opens up—precisely because of the presence of the nuclear medium [2,3]. As this ''nonmesonic'' mode dominates, the decay of the lambda in the nuclear medium becomes sensitive to nuclear excitations. Finally, the decay is interesting because the empirical $\Delta I = 1/2$ rule—nearly exact for the free decay—appears to be violated in the nuclear medium [4,5].

Because of simplicity, or perhaps because the weak $\Lambda N\pi$ couplings seem to be the only ones that are model independent [6,7], most—although certainly not all—nonrelativistic calculations to date have concentrated exclusively on pionlike nuclear excitations [8–12]. In this, our first, relativistic study of the decay we will proceed analogously; yet our results seem to indicate the need for the inclusion of additional nuclear excitations [6,7,13].

An important point that we will stress throughout this—and any future—publication is the need for consistency between theoretical calculations and, seemingly unrelated, experimental data. For example, pionlike modes have been studied extensively by a variety of experiments. Arguably the most complete set of experiments were performed at the neutron-time-of-flight (NTOF) facility at LAMPF [14,15]. These quasielastic $(\vec{p},\vec{n})$ measurements placed strong constraints on the (pionlike) spin-longitudinal response, by showing conclusively that the long-sought pion-condensed state does not exist. Although improving fast, the present experimental situation on hypernuclear decay is still limited [16–18]. Thus, the theoretical guidance provided by alternative experiments should not be underestimated. Indeed, in this work we compute the decay of Λ-hypernuclei using the same exact model that was used successfully in describing the spin-longitudinal response extracted from the quasielastic $(\vec{p},\vec{n})$ experiments [19].

We have organized our paper as follows. In Sec. II we develop the formalism needed to compute the in-medium decay of the Λ-hyperon. We rely strongly on the analytic structure of the nucleon and pion propagators to show that the non-mesonic component of the decay is sensitive to the spin-longitudinal response. The underlying $\Lambda N\pi$ dynamics is prescribed through an effective-Lagrangian approach. For the nucleon and lambda propagators we use a standard mean-field approximation to the Walecka model, while the pion propagator is evaluated in a random-phase approximation (RPA)—using a pseudovector representation for the πNN vertex. Our results are presented in Sec. III. Strong emphasis is placed on the dynamical quenching of the effective πNN coupling in the nuclear medium, and on the corresponding reduction of the hypernuclear widths. Finally, in Sec. IV we summarize our findings and make suggestions for future work.

II. FORMALISM

The dynamics of the lambda-nucleon-pion ($\Lambda N\pi$) system is described in terms of the following effective Lagrangian [7]:

$$\mathcal{L} = g_w \bar{\psi}_N(x)(1 + \kappa \gamma^5)\tau \cdot \pi(x)\psi_\Lambda(x) + \text{H.c.}, \qquad (1)$$

where $g_w = 2.35 \times 10^{-7}$ is the weak $\Lambda N \pi$ coupling constant and $\kappa = -6.7$ is the ratio of the parity conserving to the parity violating coupling. Note that—in accordance to the empirical $\Delta I = 1/2$ rule—the lambda-hyperon field occupies the lower entry of the two-component ''isospinor'' $\psi_\Lambda(x)$; the first entry is kept empty. This effective Lagrangian will now be used to compute modifications to the propagation of the Λ-hyperon in the nuclear medium. Specifically, the modified Λ-propagator in symmetric nuclear matter satisfies Dyson's equation [20]:

$$S(p) = S_0(p) + S_0(p)\Sigma(p)S_0(p) + \cdots$$
$$= S_0(p) + S_0(p)\Sigma(p)S(p), \qquad (2)$$

where the lambda (proper) self-energy is defined by

$$-i\Sigma(p) = 3g_w^2 \int \frac{d^4q}{(2\pi)^4}(1 - \kappa\gamma^5)G(p-q)(1 + \kappa\gamma^5)\Delta(q). \qquad (3)$$

Note that we have introduced the nucleon (G) and pion (Δ) propagators. Moreover, the factor of ''3'' in front of the integral appears as a direct consequence of the $\Delta I = 1/2$ rule—the $p\pi^-$ channel contributes twice as much as the $n\pi^0$ one.

A. Nucleon propagator

The nucleon propagator will be computed in nuclear matter using a mean-field approximation to the Walecka model [21]. Since most of the formal aspects of the derivation can be found in the textbook by Serot and Walecka [22]—as well as in many other publications—we limit ourselves to a brief review of the central issues.

In a self-consistent (or Hartree) approximation the relativistic nucleon propagator in nuclear matter may be written as

$$G(k) = (\not{k}^\star + M_N^\star)\left[\frac{1}{k^{\star 2} - M_N^{\star 2} + i\eta} + \frac{i\pi}{E_N^\star(\mathbf{k})}\right.$$
$$\left. \times \theta(k_F - |\mathbf{k}|)\delta(k^0 - E_N^{(+)}(\mathbf{k}))\right], \qquad (4)$$

where the following quantities have been introduced:

$$k^{\mu\star} \equiv (k^0 - V_N, \mathbf{k}), \quad E_N^{(\pm)}(\mathbf{k}) \equiv E_N^\star(\mathbf{k}) \pm V_N,$$

$$E_N^\star(\mathbf{k}) \equiv \sqrt{\mathbf{k}^2 + M_N^{\star 2}}. \qquad (5)$$

Note that once the Fermi momentum k_F is specified, the effective nucleon mass $M_N^\star$, the energy shift V_N—and with them the full nucleon propagator—can be determined [22]. The three independent parameters of the Walecka model are the mass of the scalar meson, and the scalar and vector couplings, respectively (the vector mass is kept fixed at its physical value of 783 MeV). These three parameters—which
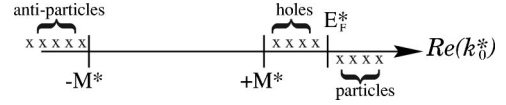
FIG. 1. Spectral content of the nucleon propagator in a relativistic mean-field approximation.

are used to describe ground-state properties of closed-shell nuclei throughout the Periodic Table—are given by

$$m_s = 520 \text{ MeV}; \quad g_s^2/4\pi = 8.724; \quad g_v^2/4\pi = 15.154. \qquad (6)$$

The above nucleon propagator can be written alternatively in a spectral representation. That is, $G(k) \equiv G^{(+)}(k) + G^{(-)}(k)$, where

$$G^{(+)}(k) = \sum_s \left(\frac{\theta(k_F - |\mathbf{k}|)}{k^0 - E_N^{(+)}(\mathbf{k}) - i\eta} + \frac{\theta(|\mathbf{k}| - k_F)}{k^0 - E_N^{(+)}(\mathbf{k}) + i\eta}\right)$$
$$\times U^\star(\mathbf{k}, s)\bar{U}^\star(\mathbf{k}, s), \qquad (7a)$$

$$G^{(-)}(k) = \sum_s \frac{V^\star(-\mathbf{k}, s)\bar{V}^\star(-\mathbf{k}, s)}{k^0 + E_N^{(-)}(\mathbf{k}) - i\eta}. \qquad (7b)$$

We have chosen to display the analytic structure of the nucleon propagator to highlight the relevant physics that has been included at the mean-field level. For example, the $G^{(-)}$ term represents the antiparticle (or filled Dirac sea) contribution to the nucleon propagator. This term is analytic in the full complex k^0-plane, except for the presence of negative-energy poles located (slightly) above the real axis. This component of the propagator does not contribute to the width of the Λ-hyperon in the nuclear medium. The $G^{(+)}$ term, in contrast, represents the positive-energy part of the propagator. In addition to a change in the dispersion relation because of the presence of the mean fields, the only other modification to this part of the propagator, relative to its free-space structure, is the shift in the position of the pole of all the states below the Fermi level from slightly below to slightly above the real k^0-axis (see Fig. 1). In this way, the ''quasi-nucleon'' propagator takes a form analogous to the one in free space—the conventional Feynman propagator—while at the same time enforcing the Pauli-exclusion principle.

B. Pion propagator I

Isolating the analytic structure of the pion propagator in nuclear matter is not as straightforward as in the case of the above nucleon propagator. Thus, in this case it is convenient to express the pion propagator in its more general form—by using its Lehmann representation [20]:

$$\Delta(q) = \frac{1}{\pi}\int_0^\infty d\omega \frac{\mathcal{I}_m\Delta(\mathbf{q}, \omega)}{\omega - q^0 - i\eta} - \frac{1}{\pi}\int_{-\infty}^0 d\omega \frac{\mathcal{I}_m\Delta(\mathbf{q}, \omega)}{\omega - q^0 + i\eta}. \qquad (8)$$

In this form, knowledge of the spectral weight (i.e., the imaginary part of the propagator) is sufficient to reconstruct

the full propagator, albeit at the expense of introducing an additional integral. Yet the virtue of such a representation is that the physical content of the imaginary part is simple and illuminating. We will return to this point later in the section. Now we proceed to compute directly the imaginary part of the lambda self-energy.

C. Lambda self-energy

As the lambda propagates through the nuclear medium it feels the presence of the strong scalar and vector mean fields. Thus, the lambda propagator gets modified at the mean-field level in a manner similar to that of the nucleon propagator. However, because there are no preexisting lambdas in the nucleus, there is no Pauli correction to the propagator. Hence, the lambda propagator looks exactly as a conventional Feynman propagator

$$S(p) = \frac{\rlap{/}{p}^\star + M_\Lambda^\star}{p^{\star 2} - M_\Lambda^{\star 2} + i\eta},\tag{9}$$

but with a mass and a dispersion relation modified by the strong mean fields:

$$p^{\mu\star} \equiv (p^0 - V_\Lambda, \mathbf{p}), \quad E_\Lambda^{(\pm)}(\mathbf{p}) \equiv E_\Lambda^\star(\mathbf{p}) \pm V_\Lambda,$$

$$E_\Lambda^\star(\mathbf{p}) \equiv \sqrt{\mathbf{p}^2 + M_\Lambda^{\star 2}}.\tag{10}$$

The only two parameters that remain to be specified are the coupling constants of the lambda to the scalar and vector fields. Here we determine them from the assumption that the strange quark in the lambda does not couple to the sigma nor to the omega meson. In this way we end up with the simple quark-model estimates of

$$g_{\sigma\Lambda\Lambda}/g_{\sigma NN} = g_{\omega\Lambda\Lambda}/g_{\omega NN} = 2/3.\tag{11}$$

Of course other possible values—perhaps phenomenologically more robust—can be easily incorporated in our calculation. Yet, irrespective of these values the effective lambda parameters become

$$(M_\Lambda^\star - M_\Lambda) = \left(\frac{g_{\sigma\Lambda\Lambda}}{g_{\sigma NN}}\right)(M_N^\star - M_N); \quad V_\Lambda = \left(\frac{g_{\omega\Lambda\Lambda}}{g_{\omega NN}}\right)V_N.\tag{12}$$

In a mean-field approximation it is the strong scalar field that is responsible for inducing a shift in the mass of the lambda, relative to its free-space value. Yet, its entire decay width is generated from the weak matrix element given in Eq. (3); note that the dispersive contribution to the mass term is insignificant. Moreover, the contribution to the width comes entirely from the particle $(+i\eta)$ component of the nucleon propagator [the last term in Eq. (7a)]. This in turn constrains the contribution from the pion propagator to arise exclusively from the first $(-i\eta)$ term in Eq. (8); otherwise the q^0 integral in Eq. (3) would vanish. In this way, the q^0 integral can be computed with the aid of Cauchy's theorem. We obtain

$$\mathcal{I}_m\Sigma(p) = 3g_w^2 \int \frac{d^3q}{(2\pi)^3}$$

$$\times \frac{(1 - \kappa\gamma^5)(\rlap{/}{k}^\star + M_N^\star)(1 + \kappa\gamma^5)}{E_N^\star(\mathbf{k})} \theta(E_N^\star(\mathbf{k}) - E_F^\star)$$

$$\times \int_0^\infty d\omega\, \mathcal{I}_m\Delta(\mathbf{q}, \omega)\delta(E_\Lambda^{(+)}(\mathbf{p}) - E_N^{(+)}(\mathbf{k}) - \omega),\tag{13}$$

where now $k^{\mu\star}$ is evaluated at its on-shell value: $k^{\mu\star} = [E_N^\star(\mathbf{k}), \mathbf{k} \equiv \mathbf{p} - \mathbf{q}]$. To proceed, and in particular to isolate the Lorentz structure of the self-energy, it is convenient to use the following identity between gamma matrices:

$$(1 - \kappa\gamma^5)(\rlap{/}{k}^\star + M_N^\star)(1 + \kappa\gamma^5)$$

$$= (1 - \kappa^2)M_N^\star + (1 + \kappa^2)\rlap{/}{k}^\star + 2\kappa\rlap{/}{k}^\star\gamma^5.\tag{14}$$

Note that a parity-violating—axial-vector—component has been generated at the one-loop level. Although interesting, the effect of this term to the decay will be of $\mathcal{O}(g_w^4)$ and will be neglected henceforth. In this way we arrive at the following form of the Λ-propagator:

$$S(p) = \frac{A_0\gamma^0 - A_v\boldsymbol{\gamma}\cdot\hat{\mathbf{p}} + B}{A_0^2 - A_v^2 - B^2},\tag{15}$$

where the following quantities have been introduced:

$$A_0 \equiv p^{0\star} - \Sigma_0,\tag{16a}$$

$$A_v \equiv |\mathbf{p}| - \Sigma_v,\tag{16b}$$

$$B \equiv M_\Lambda^\star + \Sigma_s.\tag{16c}$$

All these quantities depend (for an on-shell lambda) on the momentum of the lambda ($\mathbf{p}$) and the density of the system (k_F); for simplicity, reference to these parameters has been suppressed. The medium-modified width of the Λ-hyperon is now extracted by evaluating the imaginary part of the denominator in Eq. (15) at the position of the pole. That is,

$$\Gamma_\Lambda = -2\mathcal{I}_m\left(\frac{E_\Lambda^\star(\mathbf{p})}{M_\Lambda^\star}\Sigma_0 - \frac{|\mathbf{p}|}{M_\Lambda^\star}\Sigma_v + \Sigma_s\right).\tag{17}$$

Since in our model the medium-modified pion propagator depends solely on the magnitude and not on the direction of $\mathbf{q}$, the delta function in Eq. (13) serves to perform the angular integrations. This results in the following form for the imaginary part of the Λ-self-energy:

$$\mathcal{I}_m\Sigma_i(\mathbf{p}) = -\frac{3g_w^2}{8\pi|\mathbf{p}|}\int_0^\infty q\,dq \int_0^\infty d\omega\, C_i(q, \omega)$$

$$\times \left[-\frac{1}{\pi}\mathcal{I}_m\Delta(q, \omega)\right],\tag{18}$$
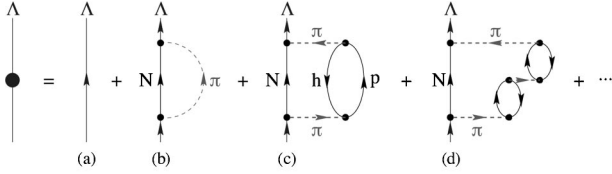
FIG. 2. Feynman diagrams contributing to the in-medium decay width of the Λ-hyperon.

where the C_i-coefficients are defined by

$$
C_i(q,\omega) = \begin{cases} (1-\kappa^2)M_N^\star, & \text{for } i=\text{S}; \\ (1+\kappa^2)E_N^\star(\mathbf{p}-\mathbf{q}), & \text{for } i=0; \\ (1+\kappa^2)(|\mathbf{p}|-\mathbf{q}\cdot\hat{\mathbf{p}}), & \text{for } i=\text{V}, \end{cases} \quad (19)
$$

supplemented with the energy-momentum-conservation relation

$$
E_N^\star(\mathbf{p}-\mathbf{q}) = \sqrt{(\mathbf{p}-\mathbf{q})^2 + M_N^{\star 2}} = E_N^{(+)}(\mathbf{p}-\mathbf{q}) - V_N
$$

$$
= E_\Lambda^{(+)}(\mathbf{p}) - \omega - V_N. \quad (20)
$$

Note that suitable kinematical conditions at the various interaction vertices impose constrains on the limits of integration for both the q- and ω-integrals in Eq. (18). For a detailed discussion on these limits we refer the reader to the Appendix.

D. Pion propagator II

Equation (18) is very general, as it depends solely on the analytic structure of the pion propagator. In this section we discuss in detail the relativistic model used to calculate the pion propagator—placing special emphasis on the physics underlying its imaginary part. The imaginary part of the pion self-energy is interesting and fundamental as it is related, after a suitable analysis, to a physical process: the (plane-wave) cross section in proton-neutron scattering. There are a variety of physical processes that modify the propagation of the pion as it moves through the many-body environment. These include the coupling of the pion to particle-hole (ph) and nucleon-antinucleon ($N\bar{N}$) excitations. In nuclear matter these two kinds of excitation have a distinctive character. For example, pions with spacelike ($q^2<0$) momenta can only ''decay'' into (real) ph-pairs. In contrast, the $N\bar{N}$-channel opens up at the relatively large timelike momentum of $q^2 = 4M_N^{\star 2} > 0$.

As was discussed in the Introduction, the mesonic decay of the lambda—in which an on-shell pion with timelike momentum is produced—is strongly Pauli-suppressed in nuclear matter [this process is represented by diagram (b) in Fig. 2]. Recall that in free space the nucleon is produced with a momentum of only 100 MeV, which is well below the Fermi momentum at saturation. However, with the closing of the mesonic branch the nonmesonic channel opens up. For this nucleon-induced ($\Lambda N \to NN$) decay the exchanged pion is constrained to have spacelike momentum. Thus, the coupling of the pion to spacelike particle-hole excitations be-

comes of paramount importance [this channel is represented by diagram (c) in Fig. 2]. We now compute the medium-modified pion propagator in nuclear matter by iterating—to infinite order—the lowest-order contribution to the self-energy by means of Dyson's equation [20]. That is,

$$
\Delta(q) = \Delta_0(q) + \Delta_0(q)\Pi_0(q)\Delta(q)
$$

$$
= \Delta_0(q) + \Delta_0(q)\Pi(q)\Delta_0(q), \quad (21a)
$$

$$
\Pi(q) = \Pi_0(q) + \Pi_0(q)\Delta_0(q)\Pi(q)
$$

$$
= \Pi_0(q) + \Pi_0(q)\Delta(q)\Pi_0(q), \quad (21b)
$$

where we have introduced the free pion propagator

$$
\Delta_0(q) = \frac{1}{q^2 - m_\pi^2 + i\eta}, \quad (22)
$$

and the lowest-order pion self-energy

$$
i\Pi_0(q) = \lambda f_\pi^2 \left(\frac{q_\mu}{m_\pi}\right)\left(\frac{q_\nu}{m_\pi}\right) \int \frac{d^4k}{(2\pi)^4}
$$

$$
\times \text{Tr}[\gamma^\mu\gamma^5 G(k+q)\gamma^\nu\gamma^5 G(k)]. \quad (23)
$$

The factor of $\lambda = 2$ represents the isospin degeneracy in symmetric nuclear matter and $f_\pi^2/4\pi = 0.0778$ represents the strength of the pseudovector πNN vertex. Further, we have established the equivalence between various ways of computing the medium-modified pion propagator. It is the last form in Eq. (21a) that we use here to write the mesonic and nonmesonic contribution to the lambda self-energy:

$$
\mathcal{I}_m\Sigma_i(\mathbf{p})|_\text{M} = -\frac{3g_w^2}{8\pi|\mathbf{p}|}\int_{q_\text{min}}^{q_\text{max}} q\, dq \int_{\omega_\text{min}}^{\omega_\text{max}} d\omega\, C_i(q,\omega)
$$

$$
\times \left[-\frac{1}{\pi}\mathcal{I}_m\Delta_0(q,\omega)\right], \quad (24a)
$$

$$
\mathcal{I}_m\Sigma_i(\mathbf{p})|_\text{N.M.} = -\frac{3g_w^2}{8\pi|\mathbf{p}|}\int_{q_\text{min}}^{q_\text{max}} q\, dq
$$

$$
\times \int_{\omega_\text{min}}^{\omega_\text{max}} d\omega\, C_i(q,\omega)\Delta_0^2(q,\omega)S_L(q,\omega).
$$

$$
(24b)
$$

Note that we have introduced the spin-longitudinal response $S_L(q,\omega)$, to be defined below. The imaginary part of the lambda self-energy is obtained by ''cutting'' all the Feynman diagrams given in Fig. 2, or equivalently, by putting all intermediate particles on their mass shell. All of these diagrams contain a nucleon in the intermediate state that must lie above the Fermi surface. Certain diagrams [such as diagram (b)] have a pion in the intermediate state and contribute to the mesonic component of the decay. However, as the mesonic component is known to be strongly suppressed by the Pauli exclusion principle, no effort has been made to compute modification to the pion mass in the nuclear me-

TABLE I. Single-particle binding energies (in MeV) for a nucleon or a lambda in the self-consistent mean-field of ^{40}Ca. Quark-model estimates were used for $g_{\sigma\Lambda\Lambda}$ and $g_{\omega\Lambda\Lambda}$. See text for details.

Orbital	N	Λ
$s^{1/2}$	−55.390	−36.274
$p^{3/2}$	−38.903	−24.030
$p^{1/2}$	−33.181	−23.591
$d^{5/2}$	−22.751	−11.769
$s^{1/2}$	−14.389	− 9.838
$d^{3/2}$	−13.876	−11.099

dium [note that even in the chiral ($m_\pi = 0$) limit the momentum of the outgoing nucleon will increase to only 160 MeV; still well below the Fermi momentum at saturation]. The decay of the lambda into a nucleon and a (spacelike) particle-hole excitation [such as in diagram (c)] constitutes the non-mesonic component of the decay. In this manner, the non-mesonic component becomes proportional to the imaginary part of the lowest-order pion self-energy, or equivalently, to the spin-longitudinal response:

$$S_L^{(0)}(q,\omega) = -\frac{1}{\pi}\mathcal{I}_m\Pi_0(q,\omega). \tag{25}$$

Finally, diagrams such as in Fig. 2(d) contribute to the nonmesonic decay through the higher-order iteration of the lowest-order pion self-energy. These diagrams have been summed to all orders using an RPA approach. Note that for the residual interaction we have included a phenomenological Landau-Migdal term, as described in detail in Ref. [19].

III. RESULTS

This section is devoted to the discussion of our results. Before doing so, however, we clarify the various approximations required to extend our nuclear-matter results to finite nuclei.

The first step in such a procedure is to calculate the ground state of various closed-shell nuclei (such as ^{40}Ca) in a relativistic mean-field approximation to the Walecka model [21,22]. Once the self-consistent mean fields are generated, we solve the Dirac equation for a Λ-hyperon moving in these potentials; no additional self-consistency is demanded. Hence, the lambda moves in a mean-field potential that differs from the corresponding nucleon potential in only two ways. First, the scalar and vector potentials were scaled by a factor of 2/3, as the strange quark in the lambda is assumed not to couple to the sigma nor to the omega meson. Second, by assuming that the magnetic moment of the lambda is carried exclusively by the strange quark, a strong tensor mean-field potential is generated. To illustrate these modifications, we have included in Table I a comparison between the nucleon and the lambda single-particle spectra using a mean-field potential appropriate for ^{40}Ca. For the case of the $s^{1/2}$ states—which lack spin-orbit partners—the binding en-

ergy for the lambda orbitals is almost 2/3 that of the nucleon. Yet the most interesting modification is the near total dilution of spin-orbit effects in the lambda spectrum due to the strong tensor interaction.

Once the Λ-spectrum has been obtained, we compute the effective (or average) vector density sampled by a Λ-hyperon occupying the lowest ($s^{1/2}$) orbital. That is,

$$\langle\rho_v\rangle = \int d^3r\,\rho_v(r)\bar{U}_\Lambda(\mathbf{r})\gamma^0 U_\Lambda(\mathbf{r}). \tag{26}$$

This is then the nuclear-matter density that is used to compute the decay width: $\Gamma_\Lambda(\mathbf{p};\langle\rho_v\rangle)$. Finally, the Λ-hypernucleus decay width is extracted from the convolution of this expression with the momentum distribution of the lowest orbital:

$$\Gamma_\Lambda = \int \frac{d^3p}{(2\pi)^3}\Gamma_\Lambda(\mathbf{p};\langle\rho_v\rangle)\bar{U}_\Lambda(\mathbf{p})\gamma^0 U_\Lambda(\mathbf{p}). \tag{27}$$

A. Mesonic decay

Computing the mesonic component of the decay is relatively straightforward. We start by writing the free pion propagator of Eq. (22) in its spectral form

$$\Delta_0(q) = \frac{1}{2\omega_\mathbf{q}}\left[\frac{1}{\omega-\omega_q+i\eta} - \frac{1}{\omega+\omega_q-i\eta}\right];$$

$$\omega_q \equiv \sqrt{\mathbf{q}^2+m_\pi^2}. \tag{28}$$

This yields the following simple form for the mesonic component of the self-energy [Eq. (24a)]:

$$\mathcal{I}_m\Sigma_i(\mathbf{p})|_M = -\frac{3g_w^2}{16\pi|\mathbf{p}|}\int_{\omega_1}^{\omega_2}d\omega\,C_i(\omega). \tag{29}$$

Here the constant C_i introduced earlier must be evaluated at its ''on-shell'' value $\omega \equiv \omega_q$. Moreover, the limits of integration are obtained from simple kinematical considerations after using the definitions given in Eqs. (A2a), (A2b), and (A3). As the weak $\Lambda N\pi$ coupling constants have been chosen to reproduce the width of the lambda-hyperon in free space, we obtain in the limit of $k_F=0$

$$\Gamma_0 = 2.490\times 10^{-12}\ \text{MeV}. \tag{30}$$

Yet the mesonic component of the decay gets modified dramatically in nuclear matter because of strong Pauli correlations. This can be seen in Table II which shows that the mesonic component of the decay drops dramatically with baryon number. We will return to discuss these results in more detail after presenting results for the nonmesonic component of the decay.

B. Nonmesonic decay

The nonmesonic component of the decay is considerably more complicated to evaluate. Not only does one need to compute the ground state of uniform nuclear matter but, in

TABLE II. Hypernuclear decay widths in a relativistic mean-field approximation to the Walecka model. The third column contains the mesonic contribution to the decay width, while the fourth and fifth columns display the dominant nonmesonic and total decay widths, respectively. The last two columns contain the nonrelativistic results, without including the two-particle—two-hole component of the decay, as computed in Ref. [11] and in Ref. [25], respectively.

Nucleus	$\langle k_F \rangle / k_F^0$	Γ_M / Γ_0	$\Gamma_{N.M.} / \Gamma_0$	$\Gamma_{Total} / \Gamma_0$	Γ / Γ_0 [11]	Γ / Γ_0 [25]
$^{12}_{\Lambda}$C	0.991	0.112	0.413	0.525	1.76	1.07
$^{16}_{\Lambda}$O	0.956	0.099	0.497	0.596	1.78	
$^{28}_{\Lambda}$Si	1.013	0.053	0.479	0.532		1.09
$^{32}_{\Lambda}$S	1.024	0.048	0.491	0.539	—	—
$^{40}_{\Lambda}$Ca	1.000	0.023	0.544	0.567	1.79	1.08

addition, one must compute its linear (spin-longitudinal) response. The linear response of the ground state—contained in the imaginary part of the polarization insertion—requires a specific representation for the πNN vertex. In this work we have adopted a pseudovector (PV) representation. The pseudovector representation adopted here is just one of several possible choices. Indeed, we could have adopted instead a pseudoscalar (PS) representation, which is guaranteed to be equivalent on-shell. The merit of the PV representation, however, is that the correct soft-pion limit of various observables is enforced at the level of the Lagrangian density, rather than from a sensitive cancellation among various Feynman diagrams [23].

One of the most interesting results that emerged from our earlier work on the pion-nucleon system is the dynamical quenching of the πNN coupling constant in the nuclear medium [19,24]. The origin of this quenching is intimately related to the nonconservation of the nucleon axial-vector current or, equivalently, to the presence of a nucleon-mass term. That is,

$$q_\mu \bar{U}(\mathbf{p}') \gamma^\mu \gamma^5 U(\mathbf{p}) = 2 M_N \bar{U}(\mathbf{p}') \gamma^5 U(\mathbf{p}) \neq 0. \quad (31)$$

In the nuclear medium the nucleon mass is reduced—dynamically—from its free-space value because of the strong scalar field. Thus, relative to a ''nonrelativistic'' calculation, by which we mean that the potentials are small and $M_N^\star \rightarrow M_N$, it appears as if the πNN coupling constant has been effectively reduced in the medium. Moreover, this reduction is density dependent and tracks the behavior of the effective nucleon mass; namely, the quenching increases with the density of the system. This relativistic behavior was responsible for generating no pion condensation—even in the absence of short-range correlations [24]. More importantly, it described correctly [19] the behavior of various quasielastic $(\vec{p}, \vec{n})$ spin observables measured at LAMPF [14,15]. Measuring a variety of spin observables was required for the extraction of the spin-longitudinal response, which was instrumental in eliminating pion condensation as a possible new state of matter. With these results in mind, we now proceed to use the same exact relativistic model to compute the nonmesonic decay of the Λ-hyperon.

Equation (24b) suggests that once the spin-longitudinal response is obtained, computing the different Lorentz com-

ponents of the non-mesonic decay becomes straightforward. We present in Fig. 3 results for the decay width of the Λ-hyperon at a nuclear-matter density $(k_F = k_F^0)$ appropriate for $^{40}_{\Lambda}$Ca (see discussion at the beginning of the section). The momentum distribution for the lowest $(s^{1/2})$ Λ-orbital is displayed by the solid line in the figure; it is normalized so that the area under the curve—which has been multiplied by a factor of 100 for clarity—is equal to one. The other three curves in the figure display the mesonic and nonmesonic components of the decay computed in an approach that has fixed all masses to their free-space value; this is our best attempt at reproducing nonrelativistic results. The dashed curve shows the mesonic component of the decay as a func-
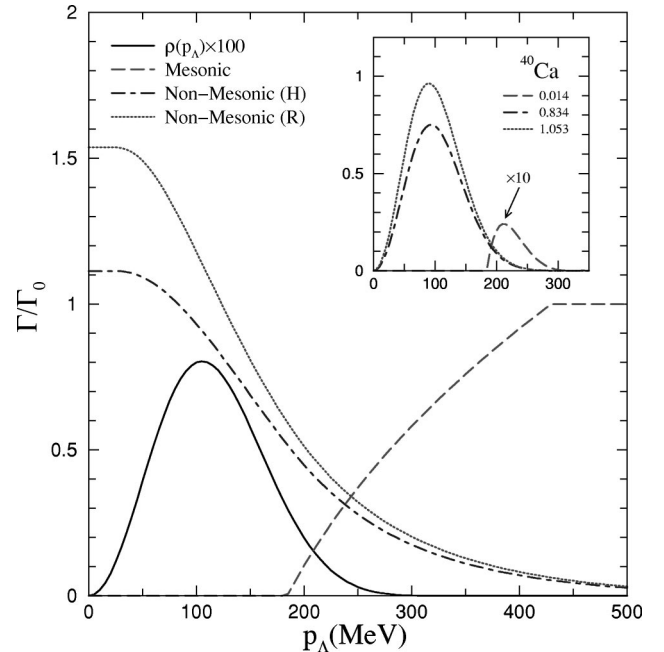
FIG. 3. Momentum dependence of the Λ-hyperon decay width, normalized to its free-space value. The mesonic contribution to the width is displayed with the dashed line, while the nonmesonic decay—with and without RPA correlations—is contained in the dotted and dot-dashed curves, respectively. All calculations were done assuming the ''nonrelativistic'' $(M_N^\star \rightarrow M_N)$ limit. The inset shows the same curves but now folded with the momentum distribution of the lowest $(s^{1/2})$ lambda orbital in $^{40}_{\Lambda}$Ca.
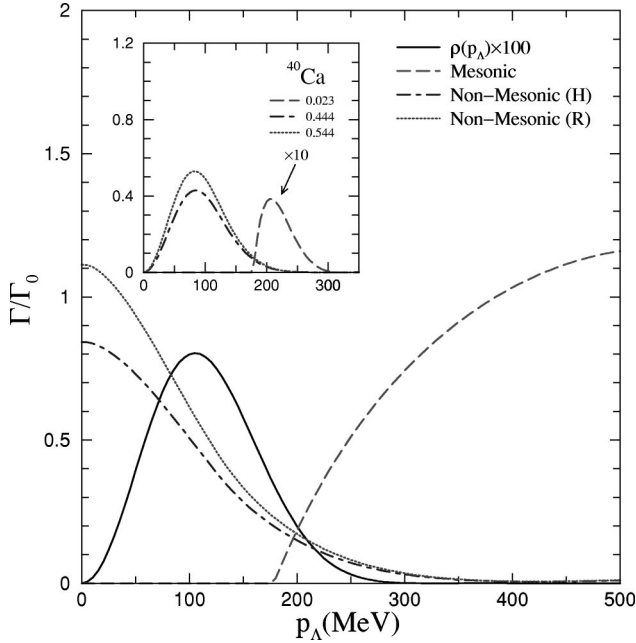
FIG. 4. Momentum dependence of the Λ-hyperon decay width, normalized to its free-space value. The mesonic contribution to the width is displayed with the dashed line, while the nonmesonic decay—with and without RPA correlations—is contained in the dotted and dot-dashed curves, respectively. All calculations were done assuming the self-consistent $(M_N^\star)$ value for the effective nucleon mass. The inset shows the same curves but now folded with the momentum distribution of the lowest $(s^{1/2})$ lambda orbital in $^{40}_\Lambda$Ca.

tion of the momentum of the lambda. Clearly, the mesonic mode is strongly suppressed for momenta below 200 MeV. The curve eventually ''heals'' to its free-space value, but too late to make a contribution to the in-medium decay; we have computed a mesonic contribution to the decay in ^{40}Ca, relative to its free-space value, of only 0.014. This number was obtained by folding the decay width computed in $(M_N^\star = M_N)$ nuclear matter with the momentum distribution of the $s^{1/2}$-orbital (see inset). The non-mesonic contributions to the decay, computed without and with RPA correlations, are displayed by the dot-dashed and dotted lines, respectively. These contributions peak at small momenta and, thus, have good overlaps with the momentum distribution. The Hartree (or non-RPA) and RPA contributions to the width have increased to 0.834 and 1.053, respectively.

The same calculation has been repeated in Fig. 4, but now with self-consistent nucleon and lambda propagators. That is, in-medium masses were used with their values determined self-consistently from the mean-field equations [22]. The different scaling of the nucleon and lambda masses with density generates a slight change in the mesonic component of the decay, but one that is still too small to impact the total decay width. By far the most important modification emerges from the dynamical quenching of the πNN coupling in the nuclear medium [24]. Indeed, the nonmesonic components of the decay computed in the relativistic approach are now reduced to 0.444 and 0.544, respectively. This large reduction factor, relative to the above $M_N^\star = M_N$ calculation, is consistent with

the reduction observed in the quasielastic $(\vec{p}, \vec{n})$ reaction [19]. Moreover, the relativistic RPA result obtained here for the total width—$\Gamma/\Gamma_0 = 0.567$—is more than a factor of three smaller than the nonrelativistic value reported by Ramos, Oset, and Salcedo in Ref. [11]. This large reduction factor is not exclusive to ^{40}Ca, but is seen in all hypernuclei reported in Table II.

It is also relevant to mention that in a very recent publication, a new nonrelativistic evaluation of the Λ-decay width has been made [25]. For the case of ^{40}Ca a total decay width (without including the two-particle—two-hole component of the decay) of $\Gamma/\Gamma_0 = 1.08$ has been reported. This represents a reduction of about 35–40 % relative to the value presented in Ref. [11]. Yet, it is essentially identical to our ''nonrelativistic'' $(M_N^\star = M_N)$ value of $\Gamma/\Gamma_0 = 1.07$. However, had we used the same $M_N^\star = M_N$ model to study the quasielastic $(\vec{p}, \vec{n})$ observables [14,15], we would have grossly overestimated the observed spin-longitudinal response [19].

We conclude this section with a brief discussion on possible improvements to our calculation. First, we have not included short-range ΛN correlations. These correlations have been found to be important in nonrelativistic calculations, as they reduce the decay width by as much as 30%. Although the inclusion of short-range correlations will only help to further strengthen our main result, namely, that the pion branch alone is not sufficient to explain the in-medium decay, their inclusion is important for a detailed comparison with experiment. Second, one should search for a phenomenologically consistent $\sigma\Lambda\Lambda$ coupling constant. For example, in a preliminary search we have found that with a small (5%) fine tuning of the coupling, one can obtain the more realistic value of 20 MeV for the binding energy of the lowest $s^{1/2}$-orbital in ^{40}Ca. This adjustment, however, results in an increase of the total decay width of only 10%. Finally, although our results for the spin-longitudinal response are in good agreement with the quasifree $(\vec{p}, \vec{n})$ data, this agreement is far from perfect—especially on the high-energy side of the quasielastic peak. Thus, a complete finite-nucleus calculation of the RPA response, similar to the one carried out for the electromagnetic response [26], should be done.

IV. CONCLUSIONS

We have computed for the first time the decay width of Λ-hypernuclei in a relativistic mean-field approximation to the Walecka model. Most of the formalism presented here is quite general, as it relies only on the analytic structure of various propagators. The calculation was performed in two stages. First, ground-state properties of various closed-shell nuclei were computed self-consistently. With the mean-fields potentials in hand, the Dirac equation for a Λ-hyperon was solved with scaled scalar and vector potentials. A scaling factor of 2/3 was introduced from the assumption that the strange quark in the lambda does not to couple to the sigma nor to the omega meson. Moreover, by assuming that the magnetic moment of the Λ-hyperon is carried solely by the strange quark, a tensor mean-field potential was introduced that diluted—almost completely—all spin-orbit effects. Sec-

ond, the mesonic and nonmesonic components of the decay width—with and without RPA correlations—were computed in infinite nuclear matter. The uniform nuclear-matter density was estimated from evaluating the average density sampled by a Λ-hyperon occupying the lowest ($s^{1/2}$) orbital. Finally, the nuclear-matter results were folded with the momentum distribution of the lowest Λ-orbital to compute the finite-hypernuclear width.

As expected, the mesonic component of the decay was strongly suppressed by Pauli correlations. Indeed, for the values of the nuclear-matter density adopted here, the decay of Λ-hyperons with momenta less than 200 MeV was strictly forbidden. Since in the Walecka mean-field model the momentum components of the Λ-hyperon beyond 200 MeV are small, the strong suppression of the mesonic mode ensued. In contrast, the nonmesonic component of the decay is not Pauli-blocked. In the nonmesonic mode the Λ-hyperon decays into a nucleon and a pionlike pair with spacelike momenta. Information on these kind of pionlike excitations is contained in the nuclear spin-longitudinal response. This fundamental nuclear response is accessible through charge-exchange $(\vec{p},\vec{n})$ reactions. Indeed, high-precision measurements made at the NTOF facility at LAMPF were instrumental in answering some fundamental nuclear-physics questions [14,15]. For example, these experiments showed conclusively, by extracting the spin-longitudinal response, that the long-sought pion-condensed state does not exist. In our relativistic model the absence of pion condensation was attributed to a dynamical quenching of the πNN coupling constant in the nuclear medium [19,24].

In the present work we have computed the nonmesonic component of the decay—using the same relativistic RPA model that was used to confirm the LAMPF measurements. The dynamical quenching of the πNN coupling constant in the medium was now responsible for generating decay widths for Λ-hypernuclei that were two to three times smaller than those obtained by existing nonrelativistic calculations [11,25]—and considerably smaller than measured experimentally [17]. This suggests that other modes of excitation, besides pionlike modes, might be important in understanding the decay width of Λ-hypernuclei [6,7,13].

The study of such modes seems both interesting and necessary. For example, a weak $\Lambda N\omega$ vertex will induce a coupling to isoscalar-vector modes. As in the pion case, this additional contribution to the nonmesonic width can be related to a well-known nuclear response: the longitudinal response measured in electron scattering. Hence, its impact on the decay will be also strongly constrained. Searching for the underlying dynamics behind the decay width of Λ-hypernuclei—while at the same time maintaining consistency with the wealth of existing nuclear-response data—will be the subject of a future report.

APPENDIX: KINEMATICAL CONSTRAINTS AT THE VERTICES

The limits of integration in the q- and ω-integrals of Eqs. (24a) and (24b) are constrained by energy-momentum conservation at the various interacting vertices. We now examine the kinematical constraints imposed at each vertex separately.

1. Kinematical constraints at the lambda-nucleon-pion vertex

Energy-momentum conservation at the $\Lambda N\pi$ vertex demands that an on-shell lambda-hyperon ''decays'' into an on-shell nucleon—above the Fermi surface—and, in principle, an off-shell pion. That is,

$$\omega = E_{\Lambda}^{(+)}(\mathbf{p}) - E_{N}^{(+)}(\mathbf{p}-\mathbf{q}) \geqslant 0. \tag{A1}$$

Moreover, as the angular integration over $\mathbf{q}$ can always be performed, the following limits of integration ensue:

$$\omega_{min} = E_{\Lambda}^{(+)} - \max(E_{N}^{(+)}(k_F), E_{N}^{(+)}(p+q)), \tag{A2a}$$

$$\omega_{max} = E_{\Lambda}^{(+)} - \max(E_{N}^{(+)}(k_F), E_{N}^{(+)}(p-q)), \tag{A2b}$$

where $E_{N}^{(+)}(p\pm q) = \sqrt{(|\mathbf{p}|\pm q)^2 + M_N^{\star 2}} + V_N$. Note that the above relations impose constraints on the q-integral as well. For example, the ω-integral will vanish unless $\omega_{max} > \omega_{min}$. Further, ω_{min} is constrained to be greater than or equal to zero. Thus, from these two conditions the following limits are obtained:

$$q_{min} = \max(0, k_F - |\mathbf{p}|),$$

$$q_{max} = \max(0, \sqrt{(E_{\Lambda}^{(+)} - V_N)^2 - M_N^{\star 2}} - |\mathbf{p}|). \tag{A3}$$

2. Kinematical constraints at the particle-hole-pion vertex

In the case of the nonmesonic decay of the lambda-hyperon, additional constraints—at least in nuclear matter—follow from enforcing energy-momentum conservation at the $ph\pi$ vertex. Indeed, the energy of the exchanged (spacelike) pion is given by

$$\omega = E_{N}^{(+)}(\mathbf{k}+\mathbf{q}) - E_{N}^{(+)}(\mathbf{k}) \geqslant 0, \tag{A4}$$

where $E_{N}^{(+)}(\mathbf{k}+\mathbf{q}) > E_{N}^{(+)}(k_F)$ denotes the energy of the particle and $E_{N}^{(+)}(\mathbf{k}) < E_{N}^{(+)}(k_F)$ is the energy of the hole. As in the above case, the most stringent constraints emerge in the case in which the particle, the hole, and the pion are collinear. We obtain

$$\omega_{min} = \max(0, \sqrt{(|\mathbf{q}| - k_F)^2 + M_N^{\star 2}} - \sqrt{k_F^2 + M_N^{\star 2}}), \tag{A5a}$$

$$\omega_{max} = \sqrt{(|\mathbf{q}| + k_F)^2 + M_N^{\star 2}} - \sqrt{k_F^2 + M_N^{\star 2}}. \tag{A5b}$$

The resulting limits of integration for the ω-integral then follow from enforcing Eqs. (A2a) and (A2b) and (A5a) and (A5b) simultaneously.

[1] W. Cheston and H. Primakoff, Phys. Rev. **92**, 1537 (1953).

[2] R. H. Dalitz, Phys. Rev. **112**, 605 (1958).

[3] M. M. Block and R. H. Dalitz, Phys. Rev. Lett. **11**, 93 (1963).

[4] E. Oset and A. Ramos, Prog. Part. Nucl. Phys. **41**, 191 (1998).

[5] A. Parreño, A. Ramos, C. Bennhold, and K. Maltman, Phys. Lett. B **435**, 1 (1998).

[6] J. F. Dubach, Nucl. Phys. **A450**, 71c (1986).

[7] John F. Dubach, Geoffrey B. Feldman, Barry R. Holstein, and Lorenzo de la Torre, Ann. Phys. (N.Y.) **249**, 146 (1996).

[8] J. B. Adams, Phys. Rev. **156**, 1611 (1967).

[9] B. H. J. McKellar and B. F. Gibson, Phys. Rev. C **30**, 322 (1984).

[10] J. Nieves and E. Oset, Phys. Rev. C **47**, 1478 (1993).

[11] A. Ramos, E. Oset, and L. L. Salcedo, Phys. Rev. C **50**, 2314 (1994).

[12] W. M. Alberico, A. De Pace, M. Ericson, and A. Molinari, Phys. Lett. B **256**, 134 (1991).

[13] A. Parreño, A. Ramos, and C. Bennhold, Phys. Rev. C **56**, 339 (1997).

[14] J. B. McClelland *et al.*, Phys. Rev. Lett. **69**, 582 (1992).

[15] X. Y. Chen *et al.*, Phys. Rev. C **47**, 2159 (1993).

[16] R. Grace *et al.*, Phys. Rev. Lett. **55**, 1055 (1985).

[17] J. J. Szymanski *et al.*, Phys. Rev. C **43**, 849 (1991).

[18] H. Noumi, S. Ajimura, H. Ejiri, A. Higashi, T. Kishimoto, D. R. Gill, L. Lee, A. Olin, T. Fukuda, and O. Hashimoto, Phys. Rev. C **52**, 2936 (1995).

[19] C. J. Horowitz and J. Piekarewicz, Phys. Lett. B **301**, 321 (1993); Phys. Rev. C **50**, 2540 (1994).

[20] A. L. Fetter and J. D. Walecka, *Quantum Theory of Many Particle Systems* (McGraw-Hill, New York, 1971).

[21] J. D. Walecka, Ann. Phys. (N.Y.) **83**, 491 (1974).

[22] B. D. Serot and J. D. Walecka, Adv. Nucl. Phys. **16**, 1 (1986).

[23] T. Matsui and B. D. Serot, Ann. Phys. (N.Y.) **144**, 107 (1982).

[24] J. F. Dawson and J. Piekarewicz, Phys. Rev. C **43**, 2631 (1991).

[25] W. M. Alberico, A. De Pace, G. Garbarino, and A. Ramos, nucl-th/9902023.

[26] C. J. Horowitz and J. Piekarewicz, Phys. Rev. Lett. **62**, 391 (1989); Nucl. Phys. **A511**, 461 (1990).